

ABSORPTION CROSS-SECTION OF DILATON-AXION BLACK HOLES

Tanwi GHOSH

Ranaghat College, Department of Physics,
District – Nadia, Pin – 741201, India
E-mail: tanwi68@gmail.com

Abstract. The expression for absorption cross-section of massless as well as massive charged particles in the background of dilaton-axion black hole is determined in low and high frequency limits. The modification of the absorption cross-section in comparison to Reissner-Nordstrom black hole is discussed.

Keywords: absorption cross-section, super-radiance, high frequency limit, low frequency limit.

1. INTRODUCTION

The study of black holes both from theoretical as well as observational point of view has emerged as a very challenging area in the context of modern astronomy and theoretical physics [1, 2]. The recent developments on experimental work in the context of Sgr.A* and M87 predict the existence of the super-massive black holes [3, 4]. The LIGO scientific collaboration reported a characteristic ‘chirp’ of gravitational waves from merger [5, 6] of binary black holes systems, providing a strong evidence of the existence of black holes. The Event Horizon team having radio-telescope of resolving power three orders of magnitude stronger than Hubble telescope seeks to observe black hole shadow [3, 7]. They have produced very recently first images of supermassive black holes M87 [5, 8, 9] at the center of galaxy. The nature of Sgr. A* is still unknown due to strong interstellar scattering which occurs at cm wavelength. Recent works on scattering and absorption of particles and waves in the black-holes background space-time have also revealed the relevance of experimental observations. In this context, the absorption of massive or massless scalar field, fermions, electromagnetic and gravitational wave in the Schwarzschild space-time has been studied [10–13]. In the background of Reissner-Nordstrom, rotating and regular black hole space-time, considerable amount of works exist in the literature [14–23]. The particle emission by black holes has also been extensively explored in the literature [24, 25]. The study of particle emission rate as well as Hawking radiation has become more significant in this regard. Besides that the absorption of matter fields by black holes has also took very important role in elucidating accretion phenomena in galactic nuclei [26–28]. The black hole absorption phenomena also revealed the fact that the high frequency limit absorption cross-section has correlation with black hole shadows.

We here thus try to analyse the features of absorption cross-section for a monochromatic planar wave of massive charged scalar particles as well as massless particles in the background of dilaton-axion black holes in low frequency as well as high frequency limit [29]. We also compare our results with Reissner-Nordstrom black holes and draw our conclusion regarding two kinds of black holes.

Our study is due to the fact that the presence of dilaton field drastically changes the distinct features which are different from other black holes. Moreover, such black holes are interesting to study because the dynamical modulus or dilaton fields coupled to string curvature may dominate the fate of dark energy dominated universe [30]. The energy density of dilaton field may influence our accelerating universe [31].

Apart from the dilaton scalar, the other scalar which appears in string inspired gravity models has implications to overcome the enigma of dark matter [32, 33].

2. THE MODEL

The action describing dilaton-axion black hole can be expressed as [29],

$$S = \int d^4x \sqrt{-g} \left[\frac{1}{2\kappa} \left(R - \frac{1}{2} \partial_\mu \varphi \partial^\mu \varphi - \frac{1}{2} e^{2a\varphi} \partial_\mu \zeta \partial^\mu \zeta \right) - e^{-a\varphi} F_{\mu\nu} *F^{\mu\nu} \right], \quad (1)$$

where R is the scalar curvature, $\kappa = 8\pi G$ be the gravitational constant in four dimension, $F^2 = F_{\mu\nu} F^{\mu\nu}$ represents Maxwell field, $*F^{\mu\nu}$, φ and ζ are the (Hodge) dual Maxwell field strength, massless scalar dilaton and the massless pseudo-scalar axion respectively. a and b represent the coupling of dilaton and axion field with electromagnetic field. We begin with the spherically symmetric metric,

$$ds^2 = -U(r) dt^2 + \frac{1}{U(r)} dr^2 + p(r)^2 d\Omega^2. \quad (2)$$

Using the action described by equation (1), two cases have been discussed [29]. Considering $|b| \neq |a|, b \ll 1$ and $a = 1$ the following metric has been derived,

$$U(r) = \left[\frac{(r - r_+)(r - r_-)}{r^2 - r_0^2} \right], \quad (3)$$

with

$$p(r)^2 = (r^2 - r_0^2). \quad (4)$$

r_+ and r_- are the two horizons and r_0 is the dilaton-axion charge. r_0 and r_\pm are related to electric charge Q_e , magnetic charge Q_m , dilaton field at infinity φ_0 and black hole mass M as $r_0 = \frac{(Q_e^2 - Q_m^2)e^{-\varphi_0}}{2M}$, and $r_\pm = M \pm \sqrt{M^2 + r_0^2 - (Q_e^2 + Q_m^2)e^{-\varphi_0}}$ [29].

3. LOW FREQUENCY REGIME

In the background of dilaton-axion black hole for $|b| \neq |a|$, we consider a charged massive perturbing scalar field. The dynamics of the scalar field can be described by the Klein-Gordon equation as follows,

$$\left[(\nabla^\nu - iqA^\nu)(\nabla_\nu - iqA_\nu) - m_1^2 \right] \Phi = 0, \quad (5)$$

where q and m_1 are the charge and mass of the scalar field. The components of the vector potential A_0 and A_3 can be derived from F_{01} and F_{23} respectively, where

$$A_0 = \frac{Q_e}{(r + r_0)} \quad (6)$$

and

$$A_3 = -Q_m \cos\theta. \quad (7)$$

For determining the black hole absorption cross-section, we need incoming modes from null infinity. The incoming modes are basically the solutions of the radial wave equation which includes only the vector potential A_0 since A_3 component will appear in the angular part of the wave equation.

Now introducing the ansatz $\Phi = e^{-i\omega t} R(r) Y_{lm}(\theta, \phi)$ and decomposing it, one can get the radial and angular part of the wave equation both of which will be of confluent Heun type [34]. The radial wave equation can be revealed as,

$$\Delta \frac{d}{dr} \left(\Delta \frac{dR}{dr} \right) + U_1 R = 0 \quad (8)$$

where ω , l and m are the conserved energy, spherical harmonic index and azimuthal harmonic index respectively. In our case, from equation (3), (4), (6) and (7), we have $\Delta = (r - r_+)(r - r_-)$ and

$$U_1 = \frac{(r^2 - r_0^2)^2}{r^2} \left(\omega r - q Q_e \frac{r}{(r + r_0)} \right)^2 - \Delta \left((r^2 - r_0^2) m_1^2 + l(l+1) \right). \quad (9)$$

Using the coordinate transformation $\frac{dr_*}{dr} = \frac{r^2}{\Delta}$ and changing the radial function as $\tilde{R} = rR(r)$, the radial equation (8) can be explored as,

$$\frac{d^2}{dr_*^2} (rR(r)) \frac{\Delta^2}{r^4} + \frac{d}{dr} (rR(r)) \frac{d}{dr} \left(\frac{\Delta}{r^2} \right) \frac{\Delta}{r^2} + \tilde{U}_1 (rR(r)) = 0, \quad (10)$$

where

$$\tilde{U}_1 = \frac{U_1}{r^4} - \frac{\Delta}{r^3} \frac{d}{dr} \left(\frac{\Delta}{r^2} \right). \quad (11)$$

By further simplification from equations (9) and (10), we get,

$$\frac{d}{dr} \left[\frac{d}{dr} (rR) \frac{\Delta}{r^2} \right] \frac{\Delta}{r^2} + \tilde{U}_1 (Rr) = 0 \quad (12)$$

Finally, from equation (12), the radial equation becomes,

$$\frac{d^2 \tilde{R}}{dr_*^2} + \tilde{U}_1 \tilde{R} = 0, \quad (13)$$

where the domain of r_* is $(-\infty, +\infty)$. \tilde{U}_1 and \tilde{R} of equation (13) are the corresponding expressions for U_1 and R which are represented in new coordinate transformation.

Introducing a new radial function $\Psi = \Delta^{\frac{1}{2}} R$ in (8), the wave equation can be expressed as,

$$\frac{d^2 \Psi}{dr^2} + (\omega^2 - V) \Psi = 0 \quad (14)$$

where the effective potential V is

$$V = \omega^2 - \frac{1}{\Delta^2} \left[U_1 + \frac{1}{4} (r_+ - r_-)^2 \right]. \quad (15)$$

In this work, we make use of a dimensionless parameter ν corresponding to the scalar-field as,

$$\nu = \sqrt{1 - \frac{m_1^2}{\omega^2}} \quad (16)$$

where υ commensurates to the ratio of speed of propagation of the wave in the far region to the speed of light. For unbound modes of the scalar field $0 < \upsilon < 1$ implies $\omega > m_1$.

From equation (16) we have,

$$m_1^2 = \omega^2 (1 - \upsilon^2). \quad (17)$$

Being $\omega > m_1$, in low frequency region, $M\omega \ll 1$ and thus $Mm_1 \ll 1$. Through m_1^2 from equation (17), we can relate υ , U_1 and V .

For $r \rightarrow r_+$, we have from equation (11),

$$\lim_{r \rightarrow r_+} \tilde{U}_1 = \left(1 - \frac{r_0^2}{r_+^2}\right)^2 \left(\omega - \frac{qQ_e}{(r_+ + r_0)}\right)^2 = \sigma^2. \quad (18)$$

Thus, the transmitted part of the radial wave equation (8) has solution as,

$$R = A_{trans} e^{-i\sigma r_*} \quad (19)$$

where A_{trans} is a constant. The coordinate r_* is represented as,

$$r_* \approx \frac{r_+^2}{(r_+ - r_-)} \ln(r - r_+) + r_*(0), \quad (20)$$

where $r_*(0)$ is a constant.

However, we want to derive the dilaton-axion black hole absorption cross-section in low frequency region considering a massive charged scalar field as a perturbing field. As we know for unbound scalar modes, $0 < \upsilon < 1$ implies $\omega > m_1$. In low frequency limit as $\omega \ll 1$, we also have $m_1 \ll 1$. On the other hand,

for massive charged scalar field ω^2 is modified by $\left(\omega - \frac{qQ_e}{r_+ + r_0}\right)^2$ in U_1 . For $qQ_e < 0$ and $\sigma > 0$, an

incoming wave will exist and super-radiance will occur. Thus, the term $\left(\omega - \frac{qQ_e}{(r_+ + r_0)}\right) \ll 1$ suggests that the

super-radiance will be absent in this case. It implies $\frac{qQ_e}{(r_+ + r_0)} \ll 1$ in low frequency limit.

In such frequency limit, one can match the behavior of Schrodinger wave function across the broad regions of black hole spacetime very accurately. Following [14], three different regions has been disposed: the region very close to the black hole horizon region, i.e. $r \approx r_+$ (region 1), an intermediate region in which

scalar field mass and frequency terms are much smaller than 1; i.e. $\omega \rightarrow 0$, $m_1 \rightarrow 0$ and $\frac{qQ_e}{(r_+ + r_0)} \ll 0$

(region 2), and a region which is far away from the black-hole horizon, i.e. $r \gg r_+$, (region 3). This is due to the fact that in low frequency limit, wave-length of the scalar field is much larger than any black hole characteristics scale.

For region 1 ($r \rightarrow r_+$). After substituting the dominating term of the expressions of r_* for region 1 for $r \rightarrow r_+$, the solution of equation (8) using equations (18), (19) and (20) can be unveiled as,

$$R_I = A_I \left(1 - i \left(\omega - \frac{qQ_e}{(r_+ + r_0)}\right) \left(1 - \frac{r_0^2}{r_+^2}\right) \frac{r_+^2}{(r_+ - r_-)} \ln(r - r_+)\right) \quad (21)$$

where A_I is a constant.

Now we find the solution in region 2. To find the solution in region 2, we take the limit $\omega \rightarrow 0$ as well as $m_1 \rightarrow 0$ in equation (8). To compute the absorption cross-section in the limit $M\omega$, $Mm_1 \ll 1$, we want to concentrate on the dominating mode $l=0$.

Now the differential equation for this region can be exhibited as,

$$\frac{d^2 R}{dr^2} - \left[\frac{(r_+ + r_- - 2r)}{(r - r_+)(r - r_-)} \right] \frac{dR}{dr} = 0. \quad (22)$$

Thus, the solution of equation (22) is

$$R_{II} = \zeta_1 \ln(r - r_+) - \zeta_1 \ln(r - r_-) + \tau. \quad (23)$$

Moreover, the equation (23) in the limit $r \rightarrow r_+$ can be represented as,

$$R_{II} = \zeta_1 \ln(r - r_+) - \zeta_1 \ln(r_+ - r_-) + \tau, \quad (24)$$

where ζ_1 and τ are constants to be determined.

Here we are seeking an overlapping in region 1 and 2. Thus, comparing the equations (21) and (24) we get

$$\zeta_1 = -A_I i \alpha \left(\omega - \frac{qQ_e}{(r_+ + r_0)} \right) \left(1 - \frac{r_0^2}{r_+^2} \right), \quad (25)$$

where $\alpha = \frac{r_+^2}{(r_+ - r_-)}$ and

$$\tau = A_I \left[1 - i \left(\omega - \frac{qQ_e}{(r_+ + r_0)} \right) \left(1 - \frac{r_0^2}{r_+^2} \right) \beta \right], \quad (26)$$

where

$$\beta = \alpha \ln(r_+ - r_-). \quad (27)$$

We now restrict ourselves in finding the solutions of region 3. For region 3 ($r \gg r_+$), the differential equation (8) using equations (14) and (15) can be disposed as,

$$\left(\frac{d^2}{dr^2} + \left[(\omega^2 - m_1^2) + \frac{2M(2\omega^2 - m_1^2)}{r} - \frac{l(l+1)}{r^2} \right] \right) \Delta^{\frac{1}{2}} R = 0. \quad (28)$$

In this equation, we neglect the terms $O\left(\frac{1}{r^2}\right)$ that are proportional to $\omega^2, m_1^2, r_0^2 m_1^2$ and terms of order $\frac{1}{r^3}$.

In the asymptotic limit for $\omega r \ll 1$ and $l=0$, the solution of equation (28) can be manifested as,

$$R_{III} = a_1 \rho \omega v + \frac{b_1}{\rho r} \quad (29)$$

where $\rho = \left(\frac{-m\omega(1+v^2)/v}{e^{-m\omega(1+v^2)/v_{-1}}} \right)$. In the asymptotic limit, the equation (24) can be expressed as,

$$R_{II} = -\zeta_1 \frac{(r_+ - r_-)}{r} + \tau. \quad (30)$$

Comparing the equations (25), (26), (29) and (30), the expressions of a_1 and b_1 can be conveyed as,

$$a_1 = \frac{A_l \left[1 - i \left(\omega - \frac{qQ_e}{r_+ + r_0} \right) \left(1 - \frac{r_0^2}{r_+^2} \right) \beta \right]}{\rho \omega \upsilon} \quad (31)$$

and

$$b_1 = A_{l\rho} (r_+ - r_-) i \alpha \left(\omega - \frac{qQ_e}{r_+ + r_0} \right) \left(1 - \frac{r_0^2}{r_+^2} \right). \quad (32)$$

On the other hand, the amplitudes for the incident and reflected waves can be exposed as,

$$A^{inc} = \left(\frac{-a_1 + ib_1}{2i} \right) \quad (33)$$

and

$$A^{ref} = \left(\frac{a_1 + ib_1}{2i} \right). \quad (34)$$

Thus, substituting a_1 and b_1 , the expressions for the amplitudes of incident and reflected waves for dilaton-axion black hole can be explored from equations (31), (32), (33) and (34) as follows,

$$A_{dilaton-axion}^{inc} = \frac{A_l \left[1 + \rho^2 \omega \upsilon (r_+ - r_-) \alpha \left(\omega - \frac{qQ_e}{r_+ + r_0} \right) \left(1 - \frac{r_0^2}{r_+^2} \right) - i \beta \left(\omega - \frac{qQ_e}{r_+ + r_0} \right) \left(1 - \frac{r_0^2}{r_+^2} \right) \right]}{2i \rho \omega \upsilon} \quad (35)$$

and

$$A_{dilaton-axion}^{ref} = \frac{\left[1 - i \left(\omega - \frac{qQ_e}{r_+ + r_0} \right) \left(1 - \frac{r_0^2}{r_+^2} \right) \beta - \upsilon \rho^2 \omega \alpha (r_+ - r_-) \left(\omega - \frac{qQ_e}{r_+ + r_0} \right) \left(1 - \frac{r_0^2}{r_+^2} \right) \right]}{2i \rho \omega \upsilon} \quad (36)$$

However, from the expressions of $A_{dilaton-axion}^{inc}$ and $A_{dilaton-axion}^{ref}$ (using equations (35) and (36)), we can derive the expression of absorption cross-section for $l = 0$ as,

$$\sigma_{abs|dilaton-axion} = \frac{\pi}{\omega^2 \upsilon^2} \frac{4\rho^2 \omega \upsilon (r_+ - r_-) \alpha \left(\omega - \frac{qQ_e}{r_+ + r_0} \right) \left(1 - \frac{r_0^2}{r_+^2} \right)}{\left[\left(1 + \rho^2 \omega \upsilon \alpha (r_+ - r_-) \left(\omega - \frac{qQ_e}{r_+ + r_0} \right) \left(1 - \frac{r_0^2}{r_+^2} \right) \right)^2 + \left(\left(\omega - \frac{qQ_e}{r_+ + r_0} \right) \left(1 - \frac{r_0^2}{r_+^2} \right) \beta \right)^2 \right]} \quad (37)$$

In the low frequency limit, using equation (37) for $\rho \approx 1$ and taking the approximation $\omega \approx 0$, the expression for absorption cross-section will reduce to the form (substituting α and β from equation (27)),

$$\sigma_{abs|dilaton-axion} = \frac{4\pi r_+^2}{\omega} \left(1 - \frac{r_0^2}{r_+^2} \right) \left(\omega - \frac{qQ_e}{r_+ + r_0} \right). \quad (38)$$

For uncharged scalar particle, the above expression (equation (38)) can be represented as,

$$\sigma_{abs|dilaton-axion} = 4\pi r_+^2 \left(1 - \frac{r_0^2}{r_+^2} \right). \quad (39)$$

Thus, comparing with the result for Reissner-Nordstrom black hole,

$$\sigma_{abs|RN} = 4\pi r_+^2 \quad (40)$$

the expression corresponding to $\sigma_{abs|dilaton-axion}$ expressed by equation (39), has been modified by the term $\left(1 - \frac{r_0^2}{r_+^2}\right)$. In Fig. 1a, σ_{abs} has been depicted for dilaton-axion black hole as well as Reissner-Nordstrom black hole using equation (40) for $Q_m = 0.5$ and $Q_m = 0$ respectively.

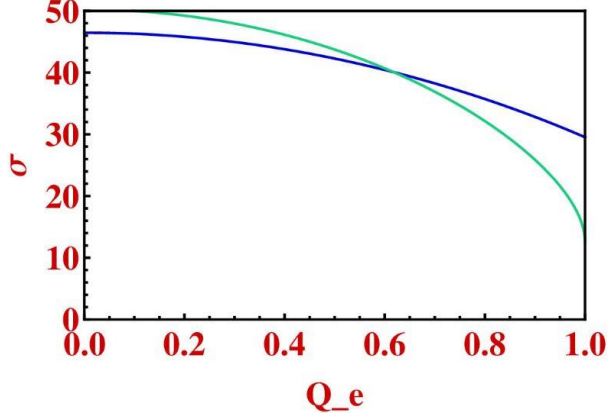


Fig. 1a – $\sigma - Q_e$ curve for Reissner-Nordstrom and Dilaton-axion black hole. Green line and Blue line correspond to $Q_m = 0$ and $Q_m = 0.5$ respectively.

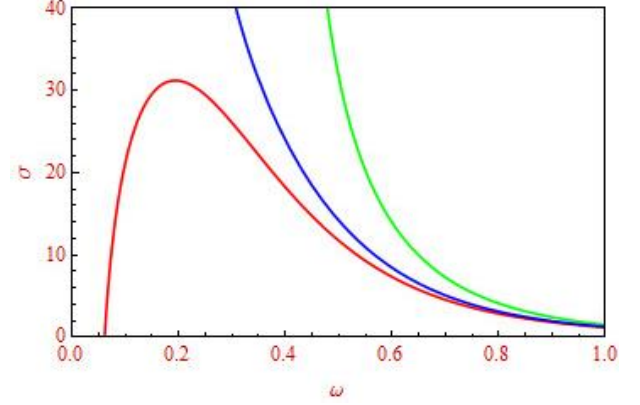


Fig. 1b – $\sigma - \omega$ curve. Red, Blue and Green line corresponds to $Mm_1 = 0.04$, $Mm_1 = 0.4$ and $Mm_1 = 0.2$ respectively.

It is explored in Fig. 1a that the curve corresponding to $Q_m = 0$ falls faster than $Q_m = 0.5$ curve. Moreover, as observed in Fig. 1b, local maxima appears for $Mm_1 = 0.04$ and black-hole charge to mass ratio, $q_1 = 0.4$ for monopole ($l = 0$) mode.

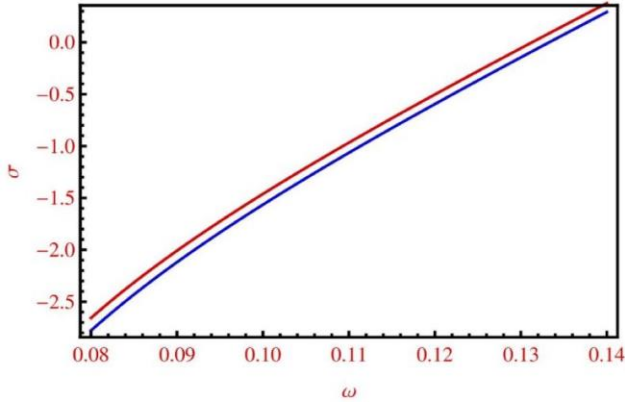


Fig. 2a – $\sigma - \omega$ curve for Reissner-Nordstrom black hole (Blue line) and Dilaton-axion black hole (Red line) for $Q = 0.6$.

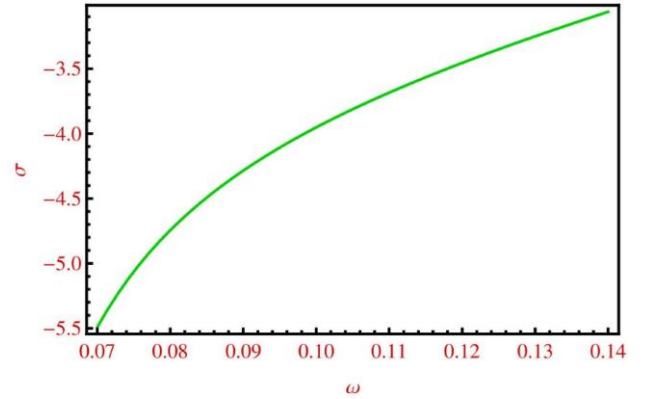


Fig. 2b – $\sigma - \omega$ curve for Dilaton-axion black hole for $Q = 1$.

However, in Fig. 2a, absorption cross-section being negative, super-radiance phenomena occurs also for dilaton-axion black holes for $Q = \sqrt{(Q_e^2 + Q_m^2)e^{-q_0} - r_0^2} = 0.6$. It is exhibited in Fig. 2b that the absorption cross-section becomes more negative with the increase of the charge of the black holes. This phenomena is similar to Kerr-Newmann black holes [35].

4. HIGH FREQUENCY REGIME

In high frequency limit, the wavelength of the scalar field turns out to be small in accordance with the horizon radius of the black hole. Thus, a wavefront can be generated along the geodesics of the black hole spacetime under eikonal approximation. The expression corresponding to the geometrical capture cross-section σ_{geo} can be explored as $\sigma_{geo} = \pi b_c^2$, where b_c represents the critical impact parameter of the unbound geodesic approaching unstable circular orbit at critical radius $r = r_c$.

Using geodesic motion and considering leading order correction, the geometrical absorption cross-section for dilaton-axion black hole can be exhibited as,

$$\sigma_{geo} = \pi \frac{\left[\left(3M + \sqrt{9M^2 - 6(Q_e^2 + Q_m^2)e^{-\varphi_0} - 2r_0^2} \right)^2 - 4r_0^2 \right]^2}{8 \left[3M^2 - (Q_e^2 + Q_m^2)e^{-\varphi_0} (Q_e^2 + Q_m^2) - 2r_0^2 \right]} . \quad (41)$$

For $r_0 = 0$, $\varphi_0 = 0$ and $Q_m = 0$, the equation (41) will reduce to the expression of Reissner-Nordstrom black-hole [36] and for $r_0 = 0$, $\varphi_0 = 0$, $Q_m = 0$ and $Q_e = 0$, it will correspond to Schwarzschild black hole.

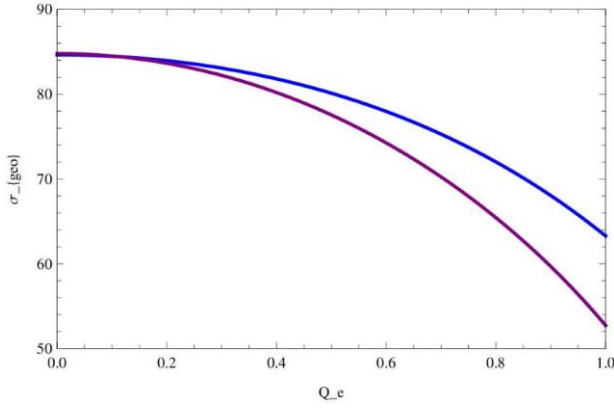


Fig. 3 – $\sigma_{geo} - Q_e$ curve for Reissner-Nordstrom black hole and Dilaton-axion black hole. Purple line and Blue line correspond to $Q_m = 0$ and $Q_m = 0.09$ respectively.

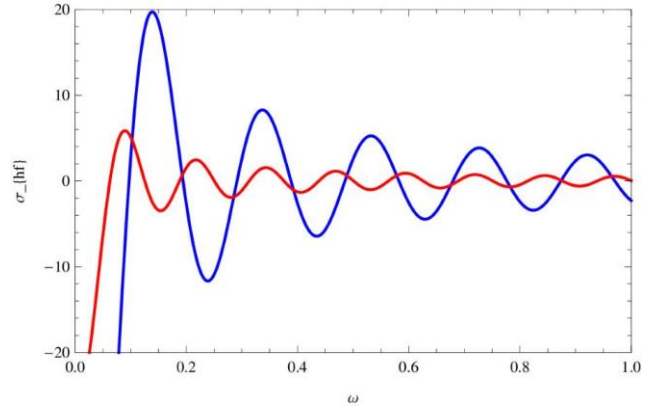


Fig. 4 – $\sigma_{abs}^{osc} - \omega$ curve for Dilaton-axion black hole. Blue line and Red line correspond to $q_1 = 0.3$ and $q_1 = 1$ respectively.

Using geometrical optics approximation, it is shown in Fig. 3, σ_{geo} vs Q_e curve for Reissner-Nordstrom black hole as well as dilaton-axion black hole taking $Q_m = 0$ and $Q_m = 0.09$ respectively. Here also the curve representing Reissner-Nordstrom black hole falls faster than dilaton-axion black hole.

At high energies, black hole absorption cross-section oscillates around a limiting constant value known as the capture cross-section or geometrical cross-section of the photon sphere [37–39]. It should be mentioned that photon sphere is a hyper-surface on which a massless particle can round the black hole under unstable circular null geodesics. Using the results for higher dimensional case, we have derived the expression of high energy oscillatory absorption cross-section for dilaton-axion black holes as,

$$\sigma_{abs}^{osc} = -8\pi\eta_c e^{-\pi\eta_c} \sigma_{geo} \text{Sinc} \left[2\pi \left(\frac{r_c}{\sqrt{U(r_c)}} \right) \omega \right] \quad (42)$$

where r_c is the radius of the unstable circular null-geodesics. The expressions of the parameter η_c and r_c can be expressed as,

$$\eta_c = \frac{1}{2} \sqrt{4U(r_c) - 2r_c^2 U''(r_c)} \quad (43)$$

and

$$r_c = \frac{\left(3(r_+ + r_-) + \sqrt{9(r_+ + r_-)^2 - 32r_+r_-}\right)}{4}. \quad (44)$$

The curves using equations (42), (43) and (44) corresponding to σ_{abs}^{osc} are shown for dilaton-axion black holes for different values of charge to mass ratio q_1 in Fig. 4. However, the Fig. 4 depicts the fact that in dilaton-axion black hole case the absorption cross-section decreases as the charge to mass ratio q_1 increases. This behavior is similar to Reissner-Nordstrom black hole as observed in [38]. Thus, it is also in concordance with the observation.

5. CONCLUSION

We study here the absorption cross-section of dilaton-axion black hole under charged massive scalar field as well as massless scalar field perturbations both in low frequency and high frequency limit considerations. It is observed that the presence of $\left(1 - \frac{r_0^2}{r_+^2}\right)$ modifies the absorption cross-section of dilaton-axion black hole in comparison to Reissner-Nordstrom black hole in low frequency limit. We further notice that σ_{abs} exhibits super-radiance effect which increases with the increase of the charge of the black holes. The increment of the value of either electric charge as well as magnetic charge decreases the absorption cross-section. Moreover, in geometrical optics approximation, we have acquired the expression of the absorption cross-section and also manifested that in absence of axion charge the absorption cross-section will reduce to the expression for Reissner-Nordstrom black hole. Thus, it is observed that in low frequency limit as well as in geometrical optics approximation, the curve corresponding to Reissner-Nordstrom black hole falls faster than dilaton-axion black hole. We have also revealed the oscillations of the absorption cross-section of dilaton-axion black holes which agree with the observations made in [39].

REFERENCES

1. K.S. THORNE, R.H. PRICE, D.A. MCDONALD, *Black holes: the membrane paradigm*, Yale University Press, 1986.
2. V.P. FROLOV, L.D. NOVIKOV (eds.), *Black hole physics: basic concepts and new developments*, 1998.
3. A. RICARTE, J. DEXTER, *The Event Horizon Telescope: exploring strong gravity and accretion physics*, Mon. Not. R. Astron. Soc., **446**, pp. 1973–1987, 2015, <https://doi.org/10.1093/mnras/stu2128>.
4. H. FAIKE, F. MELIA E. AGOL, *Viewing the shadow of the black hole at the galactic centre*, Astrophys. J., **528**, 1, art. L13, 1999, <http://dx.doi.org/10.1086/312423>.
5. R-S. LU, A.E. BRODERICK, F BARON, J.D. MONNIER, V.L. FISH, S.S. DOELEMEN, V. PANKRATIUS, *Imaging the supermassive black hole shadow and the jet base of M87 with the Event Horizon Telescope*, Astrophys. J., **788**, 2, p. 120, 2014.
6. Y. DECANINI, A. FOLACCI, M.O.E. HADJ, *How to hunt for a black hole with a telescope the size of Earth*, Phys. Rev. D, **89**, art. 084066, 2014.
7. K. AKIYAMA, K. KURAMOCHI, S. IKEDA, V.L. FISH, F. TAZAKI, M. HONMA, S.S. DOELEMEN, A.E. BRODERICK, J. DEXTER, M. MOŚCIBRODZKA, K.L. BOUMAN, *Imaging the Schwarzschild radius-scale structure of M87 with the Event Horizon Telescope using sparse modelling*, Astrophys. J., **838**, 1, p. 1, 2017.
8. Event Horizon Telescope Collaboration: K. AKIYAMA et al., *First M87 Event Horizon Telescope results VI, The shadow and mass of the central black hole*, Astrophys. J., **875**, 1, art. L6, 2019.
9. Event Horizon Telescope Collaboration: K. AKIYAMA et al., *First M87 Event Horizon Telescope results I, The shadow of the supermassive black hole*, Astrophys. J., **875**, 1, art. L1, 2019.
10. W. UNRUH, *Absorption cross-section of small black holes*, Phys. Rev. D, **14**, p. 3251, 1976.
11. E. JUNG, D. PARK, *Effect of scalar mass in the absorption and emission spectra of Schwarzschild black hole*, Classical Quantum Gravity, **21**, p. 3717, 2004.
12. C. DORAN, A. LASENBY, S. DOLAN, I. HINDER, *Fermion absorption cross-section of Schwarzschild black hole*, Phys. Rev. D, **71**, art. 124020, 2005.
13. S. DOLAN, C. DORAN, A. LASENBY, *Fermion scattering by a Schwarzschild black hole*, Phys. Rev. D, **74**, art. 064005, 2006.

14. L.C. CRISPINO, A. HIGUCHI, E.S. OLIVEIRA, *Electromagnetic absorption cross-section of Reissner-Nordström black holes revisited*, Phys. Rev. D, **80**, art. 104026, 2009.
15. K. GLAMPEDAKIS, N. ANDERSON, *Scattering of scalar waves by rotating black holes*, Classical Quantum Gravity, **18**, art. 1939, 2001.
16. R. BRITO, V. CARDOSO, P. PANI, *Black holes with massive graviton hair*, Phys. Rev. D, **88**, art. 064006, 2013.
17. C.L. BENONE, E.S. CRISPINO, A. HIGUCHI, *Absorption of a massive scalar field by a charged black hole*, Phys. Rev. D, **89**, art. 104053, 2014.
18. E.S. OLIVEIRA, L.C. CRISPINO, A. HIGUCHI, *Equality between gravitational and electromagnetic absorption cross-sections of extreme Reissner-Nordstrom black holes*, Phys. Rev. D, **84**, art. 084048, 2011.
19. L.C.S. LEITE, S.R. DOLAN, L.C.B. CRISPINO, *Absorption of electromagnetic and gravitational waves by Kerr black holes*, Phys. Lett. B, **774**, p. 130, 2017.
20. L.C.S. LEITE, C.L. BENONE, L.C.B. CRISPINO, *Scalar absorption by charged rotating black holes*, Phys. Rev. D, **96**, Art. 044043, 2017.
21. C.L. BENONE, L.C.B. CRISPINO, *Superradiance in static black hole spacetimes*, Phys. Rev. D, **93**, Art. 024028, 2016.
22. P.A. GONZALEZ, E. PAPANTONOPOULOS, J. SAAVEDRA, Y. VASQUEZ, *Superradiant instability of near extremal and extremal four dimensional charged hairy black holes in anti-de Sitter spacetime*, Phys. Rev. D, **95**, Art. 064046, 2017.
23. L.C.B. CRISPINO, S.R. DOLAN, A. HIGUCHI, E.S. OLIVEIRA, *Inferring black hole charge from backscattered electromagnetic radiation*, Phys. Rev. D, **90**, Art. 064027, 2014.
24. S.W. HAWKING, *Black hole explosions?*, Nature, **248**, pp. 30–31, 1974.
25. G.W. GIBBONS, *Vacuum polarization and the spontaneous loss of charge by black holes*, Commun. Math. Phys., **44**, pp. 245–264, 1975.
26. G.L. GRANATO, G.D. ZOTTI, L. SILVA, A. BRESSAN, L. DANESE, *A physical model for the coevolution of QSOs and their spheroidal hosts*, Astrophys. J., **600**, p. 580, 2004.
27. A. MARCONI, G. RISALITI, R. GILLI, L.K. HUNT, R. MAIOLINO, M. SALVATI, *Local supermassive black holes relics of active galactic nuclei and the X-ray background*, Mon. Not. R. Astron. Soc., **351**, pp. 169–185, 2004.
28. L. FERRARESE, H. FORD, *Supermassive black holes in galactic nuclei: past, present and future research*, Space Sci. Rev., **116**, pp. 523–624, 2005.
29. S. SUR, S. DAS, S. SENGUPTA, *Charged black holes in generalized dilaton-axion gravity*, J. High Energy Phys., **10**, Art. 064, 2005.
30. M. SAMI, A. TOPORENSKY, P.V. TRETJAKOV, S. TSUJIKAWA, *The fate of (phantom) dark energy universe with string curvature corrections*, Phys. Lett. B, **619**, pp. 193–200, 2005.
31. M. GASPERINI, *Late time effects of Planck-scale cosmology: dilatonic interpretation of the dark energy field*, In: *Thinking, Observing and Mining the Universe* (eds. G. Miele, G. Longo), Proceedings of the International Conference, Sorrento, Italy, 22–27 September 2003, pp. 153–160, 2004.
32. S. WEINBERG, *A new light boson?*, Phys. Rev. Lett, **40**, p. 223, 1978.
33. F. WILCZEK, *Problems of strong P and T in variance in the presence of instantons*, Phys. Rev. Lett, **40**, p. 279, 1978.
34. A. RONVEAUX, *Heun's differential equations*, Oxford University Press, Oxford, UK, 1995.
35. C.L. BENONE, L.C.B. CRISPINO, *Massive and charged scalar field in Kerr-Newman spacetime: Absorption and superradiance*, Phys. Rev. D, **99**, Art. 044009, 2019.
36. L.C.B. CRISPINO, E.S. OLIVEIRA, *Electromagnetic absorption cross-section of Reissner-Nordström black holes*, Phys. Rev. D, **78**, Art. 024011, 2008.
37. C.F.B. MACEDO, L.C.S. LEITE, E.S. OLIVEIRA, S.R. DOLAN, L.C.B. CRISPINO, *Absorption of planar massless scalar waves by Kerr black holes*, Phys. Rev. D, **88**, Art. 064033, 2013.
38. L.C.B. CRISPINO, S.R. DOLAN, E.S. OLIVEIRA, *Scattering of massless scalar waves by Reissner-Nordström black holes*, Phys. Rev. D, **79**, Art. 064022, 2009.
39. Y. DECANINI, G. ESPOSITO-FARESE, A. FOLACCI, *Universality of high energy absorption cross-sections for black holes*, Phys. Rev. D, **83**, Art. 044032, 2011.

Received January 11, 2022